Cell, Vol. 85, 721–732, May 31, 1996, Copyright ©1996 by Cell Press

Enhanced Growth of Mice Lacking the Cyclin-Dependent Kinase Inhibitor Function of $p27^{Kip1}$

Hiroaki Kiyokawa,* Rhonda D. Kineman,† Katia O. Manova-Todorova,* Vera C. Soares,* Eric S. Hoffman,‡ Masao Ono,* Dilruba Khanam,* Adrian C. Hayday,‡ Lawrence A. Frohman,† and Andrew Koff*

*Program in Molecular Biology
Memorial Sloan–Kettering Cancer Center
1275 York Avenue
New York, New York 10021
†Department of Medicine
University of Illinois at Chicago
Chicago, Illinois 60612
‡Department of Biology
Section of Immunobiology
Yale University
New Haven, Connecticut 06511

Summary

Disruption of the cyclin-dependent kinase–inhibitory domain of p27 enhances growth of mice. Growth is attributed to an increase in cell number, due to increased cell proliferation, most obviously in tissues that ordinarily express p27 at the highest levels. Disruption of p27 function leads to nodular hyperplasia in the intermediate lobe of the pituitary. However, increased growth occurs without an increase in the amounts of either growth hormone or IGF-I. In addition, female mice were infertile. Luteal cell differentiation is impaired, and a disordered estrus cycle is detected. These results reflect a disturbance of the hypothalamic–pituitary–ovarian axis. The phenotypes of these mice suggest that loss of p27 causes an alteration in cell proliferation that can lead to specific endocrine dysfunction.

Introduction

Activation of cyclin-dependent kinases (CDKs) regulates progression through critical transitions in the cell cycle (Sherr, 1993). CDKs contain a catalytic subunit, the CDK, and a regulatory subunit, a cyclin. Two distinct CDKs, CDK4 or CDK6 and CDK2, control entry into S phase (Ohtsubo and Roberts, 1993; Quelle et al., 1993; Resnitzky and Reed, 1995). Inactivation of either kinase leads to cessation of proliferation and withdrawal from the mitotic cycle. These G1 CDKs integrate mitogenic and anti-mitogenic signals that regulate progression through G1 to a point where further cell cycle progression continues autonomously (Pardee, 1989). This implies a capacity to regulate CDKs in response to external factors. The activation of CDKs is subject to multiple levels of regulation (reviewed by Morgan, 1995): the synthesis of the cyclin and CDK, the assembly of these proteins into complexes, the activation of these complexes, and the ability of these complexes to phosphorylate substrates. Recent work has identified two families of proteins that act as negative regulators of G1 CDKs, Inks and Cip/Kips (hereafter referred to as Kips). Inks specifically target the CDK4 and CDK6 kinases and bind to these proteins, preventing their interaction with cyclin D. In contrast, Kips bind preferentially to cyclin–CDK complexes and either prevent their activation by the CDK-activating kinase or inhibit their kinase activity. In addition, Kips, unlike Inks, are promiscuous and interact with most G1 CDKs (Sherr and Roberts, 1995).

At present, there are three members of the Kip family: p21 (Gu et al., 1993; Harper et al., 1993; Xiong et al., 1993), p27 (Polayk et al., 1994b; Toyoshima and Hunter, 1994), and p57 (Lee et al., 1995; Matsuoka et al., 1995). These proteins contain a conserved domain that is both necessary and sufficient for cyclin–CDK interaction and inhibition (Nakanishi et al., 1995). In proliferating cells, p21 and p27 associate with active CDKs (Zhang et al., 1994; Soos et al., 1996). In vitro reconstitution experiments indicate a requirement for the association of multiple molecules of Kip with a cyclin–CDK complex for complete inhibition of kinase activity (Harper et al., 1995). Amino acids 17–71 of p21 contain the cyclin–CDK-binding/inhibition domain (Nakanishi et al., 1995) and can be further divided into three subdomains: A, B, and M (Chen et al., 1996). Similar homologous domains can be postulated in p27 within amino acids 26–88: 26–51 (domain A), 69–88 (domain B), and 37–56 (domain M). Deletion analysis and site-directed mutagenesis have established the importance of the putative A and B domains (Polyak et al., 1994b; Luo et al., 1995). The function of the remaining region of p27, amino acids 92–197, is unknown at this time.

The properties of p27 suggest that it might have an important role regulating entry into and exit from the mitotic cycle. First, there is correlation between growth arrest and the amount of p27–CDK2 complex under various anti-mitogenic conditions (Koff and Polyak, 1995). Second, ectopic expression of p27 cDNA is sufficient to induce G1 arrest (Polyak et al., 1994b; Toyoshima and Hunter 1994) and, in some cells, differentiation phenotypes (Kranenburg et al., 1995; Liu et al., 1996), presumably by targeting G1 CDK activity. Third, antisense vectors targeted to p27 mRNA increase the fraction of cells in S phase (Coats et al., 1996). These properties suggest that p27 might function to establish an inhibitory threshold that G1 CDKs must surpass before activation and entry into S phase.

Consequently, a question arose as to the relevance of p27-mediated regulation of cell cycle progression to mammalian development. To determine the effect of inactivation of p27 in mammalian development, we disrupted the p27 coding region in mice and characterized the phenotypes of these animals. $p27^{-/-}$ mice grow to a greater size than controls, owing at least in part to increased cell proliferation and not to a change in the amount of either growth hormone (GH) or insulin-like growth factor I (IGF-I). There was a correlation between p27 protein expression in visceral organs and the effect of p27 disruption on the weight of the organs. These data suggest that p27 is a cell type–specific regulator of proliferation. Another phenotype of p27 disruption

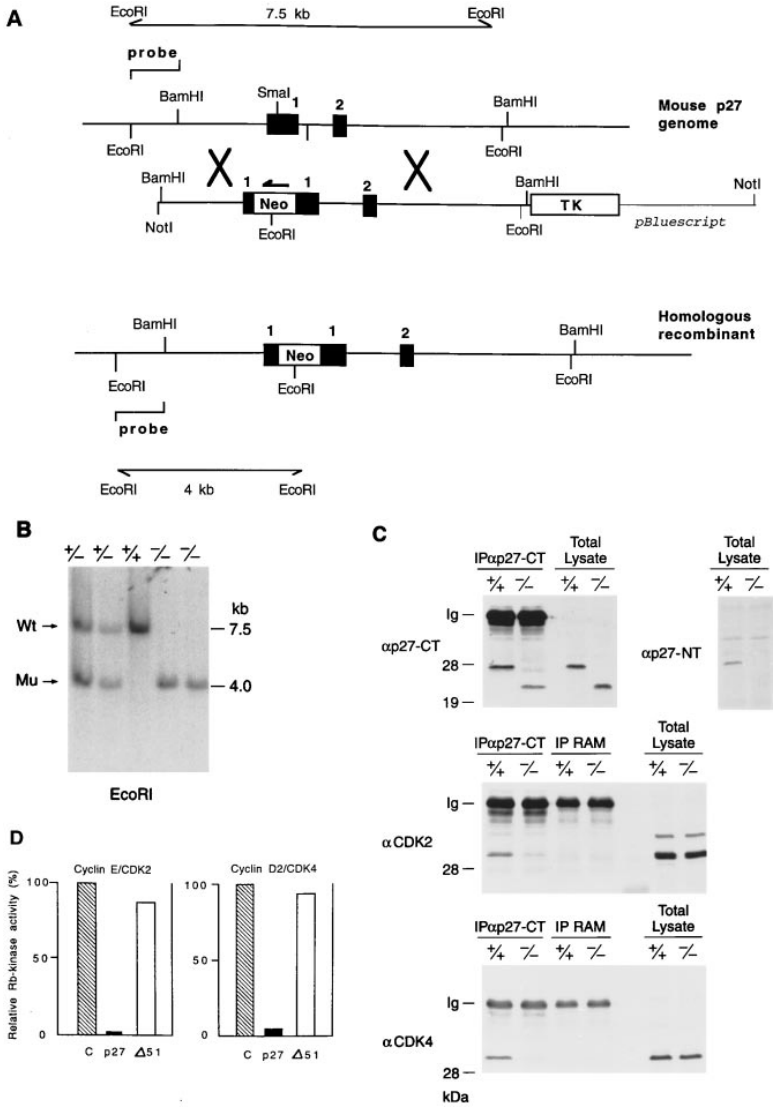

Figure 1. Targeted Insertion of the p27 Gene Produces an Amino-Terminal Truncated Protein That Does Not Inhibit G1 CDKs

(A) Restriction map of the mouse p27 gene, the targeting vector, and the structure of the locus following recombination. The targeting construct contains both coding exons of p27 with a *neo* cassette introduced into the SmaI site at amino acid 42. Transcriptional direction of the *neo* gene is shown. The TK gene is indicated to the 3′ end of the genomic sequences. Homologous recombination within the genomic sequence introduces the *neo* gene and eliminates the TK gene (Mansour et al., 1988). A single probe to the 5′ end of p27 can be used to identify recombinant alleles at 4.0 kb and wild-type alleles at 7.5 kb following EcoRI digestion of genomic DNA.

(B) Southern blot analysis of DNA from mice obtained by intercross breeding of heterozygous mice. Mice from intercross breeding were genotyped using tail DNA digested with EcoRI prior to electrophoresis using the probe in (A).

(C) Analysis of p27 protein products in $p27^{+/+}$ and $p27^{-/-}$ mouse embryonic fibroblasts. Immunoprecipitates of p27 or whole-cell lysates were subjected to SDS–polyacrylamide gel electrophoresis and immunoblotted with the antibodies indicated to the left: p27 carboxyl terminus–specific antibody (αp27-CT), p27 amino terminus–specific antibody (αp27-NT), CDK2 and CDK4 carboxyl terminus–specific antibodies (αCDK2 and αCDK4, respectively), rabbit anti–mouse immunoglobulin (RAM). Markers and the migration of the immunoglobulin heavy chain are indicated.

(D) Δ51 protein is not able to inhibit cyclin G1–CDK activity. Lysates were prepared from Sf9 cells coinfected with the baculoviruses expressing cyclin and CDK subunits indicated above each graph. Equal amounts (30 nM) of either p27 (closed bars) or Δ51 (open bars) were added, and kinase activity was measured relative to a control (hatched bars), in which neither protein was added. The kinase activity was determined on a glutathione S-transferase–Rb substrate and plotted as percentage of the control.

was female infertility. These mice had a prolonged estrus cycle, which could be due to inappropriate endocrine regulation linked to failure to produce luteal cells, hyperplasia of the intermediate lobe of the pituitary, or a combination of both. Together, these findings demonstrate that p27 is an essential regulator of body growth in mice, but with more specific endocrine effects on particular cell types. These observations suggest that a combination of alteration in cell proliferation and perturbation of specific endocrine systems causes the phenotypes of $p27^{-/-}$ mice.

Results

Targeted Mutagenesis of the Mouse p27 Gene

To investigate the function of p27 in mammalian development, we disrupted the p27 coding sequence by homologous recombination (Figure 1A). The mouse p27 protein is encoded within two exons divided at codon 159. To disrupt specifically the cyclin–CDK inhibition domain of p27, we inserted a neomycin resistance (*neo*) gene cassette into codon 42 and a herpes simplex virus thymidine kinase (TK) gene 3′ to the genomic sequences. Out of approximately 800 colonies dual resistant to G418 and ganciclovir, we expanded 80 clones and analyzed their genotypes by Southern blotting. Of these, 14 clones had a legitimate homologous recombination event in one allele of the p27 gene. To generate chimeras, we injected six of the $p27^{+/-}$ embryonic stem (ES) cell clones individually into blastocysts prepared from C57BL/6 females and transplanted the injected blastocysts to pseudopregnant females. Three of the clones transmitted to the germline, and from these we generated $p27^{+/-}$ mice (Figure 1B). Further intercross of the $p27^{+/-}$ mice produced offspring at predicted Mendelian ratios. Therefore, this targeted mutation of p27 does not affect survival during embryogenesis.

To examine whether the p27 mutant allele was capable of expressing any protein, we prepared fibroblasts from embryos (mouse embryo fibroblasts [MEFs]) and

analyzed the lysates by immunoblotting (Figure 1C). Using antibodies to either full-length p27 or the carboxyl terminus of p27, we detected a 20 kDa protein in $p27^{-/-}$ MEFs and a 27 kDa protein in $p27^{+/+}$ MEFs. Both proteins were detected in $p27^{+/-}$ MEFs (data not shown). In contrast, antibody specific to the amino terminus of p27 recognized only the 27 kDa protein and not the 20 kDa protein (Figure 1C). The amounts of the 20 kDa species and p27 were comparable. Using polymerase chain reaction, we amplified RNA transcripts from the p27 mutant allele and determined its structure; the mutant transcript had the insertion of the *neo* gene in the antisense direction and normal splicing of the intron separating exons 1 and 2. This transcript contains a predicted open reading frame that encodes amino acids 52–198 of the p27 protein (data not shown).

Taken together, the disruption of the p27 gene produced an amino-truncated mutant of p27 protein, which we call Δ51. His-tagged Δ51 purified from bacteria and added to extracts of Sf9 cells coinfected with baculoviruses expressing either cyclin E and CDK2 or cyclin D2 and CDK4 inhibited retinoblastoma protein (Rb) phosphorylation by these kinases less efficiently than the full-length p27 (Figure 1D). Furthermore, Δ51 interacted poorly with cyclin–CDK complexes in cells (Figure 1C). These results suggest that, at the amounts produced in cells, Δ51 will not inhibit G1 CDKs and will not act in a dominant-negative fashion to exclude the binding of other CDK inhibitors.

Mice Lacking Functional p27 Are Larger than Normal

Following weaning, the $p27^{-/-}$ mice weighed 20%–40% more than sex-matched littermate controls. A representative litter of male mice at 8 weeks of age is shown in Figure 2A. A comparison of male mice derived from intercross breeding suggested that the weight of the mouse was a function of the p27 gene copy number (Figure 2B). Analysis of pups from intercross breeding at the first 3 weeks postpartum indicated that the mean weight of $p27^{-/-}$ mice was generally higher than $p27^{+/+}$ mice, but there was significant overlap in the weight of each population. In 8-week-old mice the difference between the populations was much greater, and the smallest $p27^{-/-}$ mice weighed as much as the largest $p27^{+/+}$ mice ($p < 0.01$). The mean weight and range of $p27^{+/-}$ mice were intermediate. To determine the earliest time after birth at which we could detect this difference, we weighed the mice from 1 week postpartum. There were 21 suitable mice in litters in which sex-matched comparisons to controls could be made. Most of the $p27^{-/-}$ mice (71%, $n = 15$) were larger than littermate $p27^{+/+}$ controls during the first 14 days postpartum (data not shown). However, the weight of the remaining mice (29%, $n = 6$) was either less than or equal to their wild-type siblings within the first 14 days; by day 32 they weighed more. Representative growth curves of two pairs of such siblings are shown in Figure 2C.

To determine if there was a correlation between weight and growth, we examined skeletal growth and organ weight. By radiography ($n = 5$), we observed differences in the length of the skull and longitudinal bones, including the femur, tibia, and humerus, that corresponded to the increase in the size of the mouse (data not shown). To examine whether enlargement of visceral organs was also proportional to that of the mice, we measured wet weight of the brain, thymus, heart, liver, spleen, kidney, and carcass. Organ weights were consistently greater in $p27^{-/-}$ mice as compared with controls, but did not invariably increase in proportion to the weight of the animal (Figure 3A). The weight of the thymus and spleen increased the most relative to the increase in body weight. Carcass weight increased proportionally to body weight, suggesting that increases in the growth of muscle or connective tissue (or both) are partially responsible for the increased body weight (data not shown).

Since the effect of the p27 mutation on the weight of various organs varied in relation to the total body weight, we speculated that the expression and function of p27 might be tissue specific. We therefore analyzed the expression of wild-type and mutant p27 protein in the organs of $p27^{+/+}$ and $p27^{-/-}$ mice, respectively (Figure 3B). While all $p27^{+/+}$ tissues had detectable amounts of p27 protein, it was most abundant in thymus and spleen, consistent with the observation that the weight of these organs was most affected by p27 gene disruption. The expression of the truncated mutant protein in $p27^{-/-}$ mice showed a similar, although not identical, tissue specificity (Figure 3B). The biologic significance of this was not pursued in these studies. Loss of p27 did not affect tissue-specific expression of the other Kip family proteins, p21 and p57 (data not shown).

Lack of Functional p27 Leads to Hyperplasia in the Intermediate Lobe of the Pituitary

Transgenic mice expressing GH (Palmiter et al., 1982) or IGF-I (Mathews et al., 1988) grow larger than control mice. To determine if the size of the $p27^{-/-}$ mice was caused by changes of the GH–IGF-I axis, we investigated the effect of p27 gene disruption on the pituitary. In all 11-week-old mice we examined ($n = 6$), the pituitary gland appeared increased in size, with a prominent midline intermediate–posterior lobe region. Hematoxylin and eosin staining revealed intermediate lobe hyperplasia with normal cellular morphology and arrangement and normal vascularity (Figure 4A, middle). The anterior lobes appeared compressed, with increased cellular density, while the posterior lobe appeared normal. In all 30-week-old mice ($n = 3$), the intermediate lobe was even more hypercellular, with circular nests of cells giving the appearance of nodules (Figure 4B, right). A marked increase in vascularity was present throughout the lobe, manifested as lakes of distended capillaries filled with red blood cells. In some animals the tissue mass was sufficiently large as to cause compression of the ventral hypothalamus. The intermediate lobe contains cells that produce α melanocyte-stimulating hormone (αMSH). There was homogeneous staining with an antibody that reacts with proopiomelanocortin (POMC)-derived peptides, including αMSH, in the intermediate lobe cells at 11 weeks (Figure 4B). At 30 weeks, however, the staining was nonhomogeneous, with some of the nodular regions exhibiting intense staining while staining in others was markedly decreased, in some to the point of nonstaining.

To determine whether the intermediate lobe hyperplasia affected the GH–IGF-I axis, we used immunohistochemistry to detect GH in the pituitary sections. In 11-

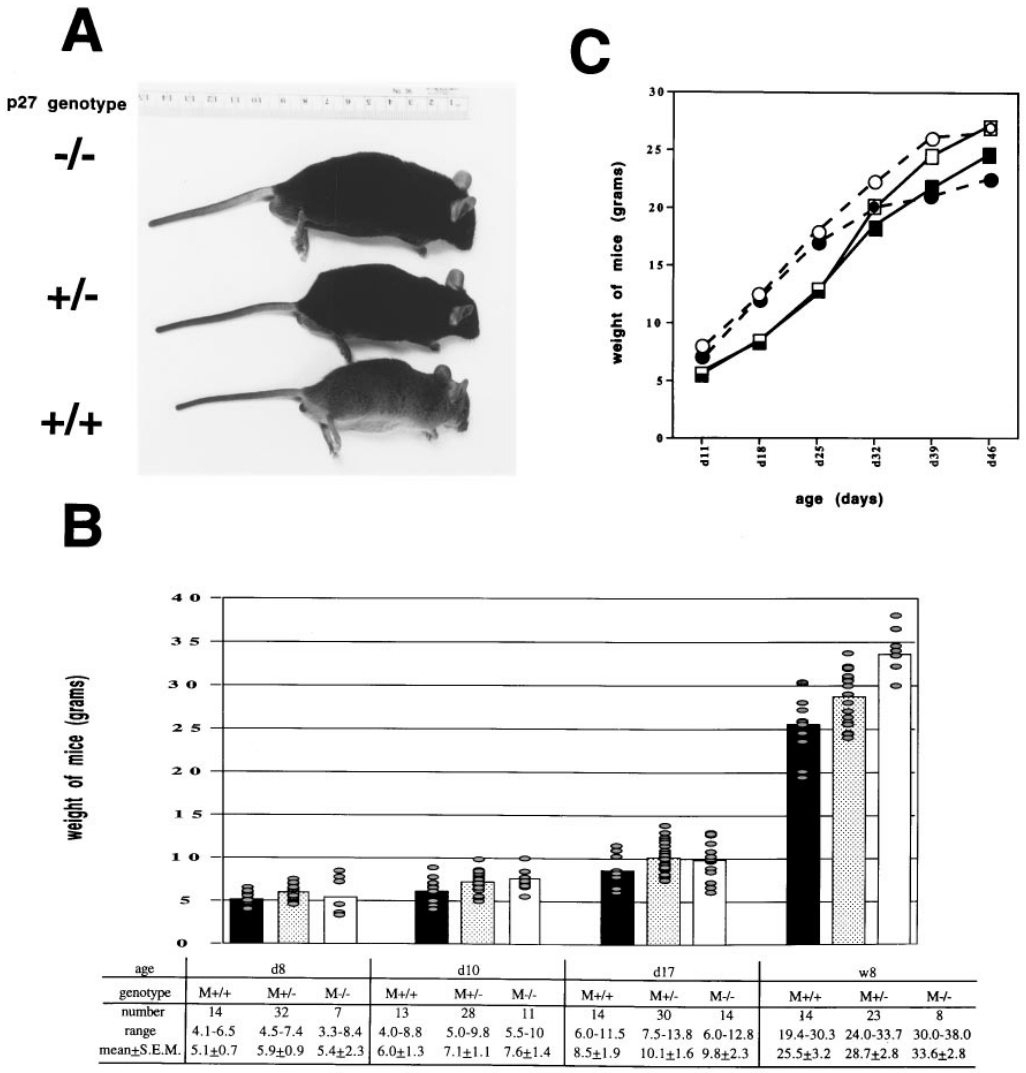

age	d8			d10			d17			w8		
genotype	M+/+	M+/-	M-/-	M+/+	M+/-	M-/-	M+/+	M+/-	M-/-	M+/+	M+/-	M-/-
number	14	32	7	13	28	11	14	30	14	14	23	8
range	4.1-6.5	4.5-7.4	3.3-8.4	4.0-8.8	5.0-9.8	5.5-10	6.0-11.5	7.5-13.8	6.0-12.8	19.4-30.3	24.0-33.7	30.0-38.0
mean±S.E.M.	5.1±0.7	5.9±0.9	5.4±2.3	6.0±1.3	7.1±1.1	7.6±1.4	8.5±1.9	10.1±1.6	9.8±2.3	25.5±3.2	28.7±2.8	33.6±2.8

Figure 2. Enhanced Growth of $p27^{-/-}$ Mice

(A) Representative picture of 8-week-old mice derived from intercross breeding of p27 heterozygous mice. Genotypes are indicated on the left.
(B) The size of mice is a function of p27 gene copy number. We conducted a retrospective analysis of weight using 252 mice obtained by intercross breeding in our colony between April and November of 1995. In the graph, the mean weight of mice is represented by bars: $p27^{+/+}$, closed bars; $p27^{+/-}$, stippled bars; $p27^{-/-}$, open bars. The actual weights of individual mice are indicated by the gray dots. The age (in days [d] and weeks [w]), genotype, numbers, and weight range of mice, as well as mean and standard deviations, are indicated. There is a statistically significant difference between the $p27^{+/+}$ and $p27^{-/-}$ groups at 8 weeks ($t = -6.110$; $p < 0.01$).
(C) Representative growth curve of two $p27^{+/+}$ and $p27^{-/-}$ littermates that were approximately the same weight within the first 2 weeks postpartum. Males are represented by the solid line and females by the broken line. $p27^{+/+}$, closed squares and circles; $p27^{-/-}$, open squares and circles.

and 30-week-old $p27^{-/-}$ mice, both the numbers of somatotropes and the intensity of GH staining were comparable with controls (data not shown). The direct assessment of GH secretion from single measurements of serum GH level is difficult because of the pulsatile nature of secretion and the influence of stress. IGF-I is the major GH-dependent postnatal growth factor. We did not find any significant genotype-dependent differences in IGF-I levels. The level of IGF-I in sera isolated from both male and female $p27^{+/+}$ mice was 36 ± 12 ng/ml, with values ranging from 19–63 ng/ml. In $p27^{-/-}$ mice, both male and female, the IGF-I levels were 34 ± 20 ng/ml, with values ranging from 5–64 ng/ml. When comparing measurements on a sex-matched basis, we find less variation in the amounts of serum IGF-I. These results indicate that the enhancement of postnatal body growth in the $p27^{-/-}$ mice is independent of the regulation by the GH–IGF-I hormonal system.

p27 Disruption Increases the Number of S Phase Thymocytes

The disruption of p27 might affect the proportion of proliferating cells in a tissue before maturation. In most specialized cell types of the animal, the proliferative index decreases following birth; however, thymocytes are still in the process of expansion and can be used

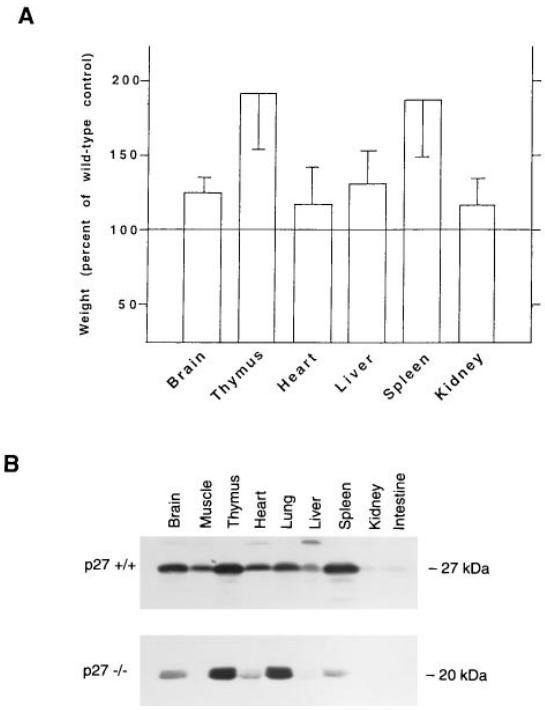

Figure 3. There Is a Correlation between Expression of p27 Protein in an Organ and the Increase in Weight of the Organ Following p27 Gene Disruption

(A) Relative organ weight in $p27^{-/-}$ mice. Organs were dissected and weighed; results are expressed as weight relative to weight of controls from age- and sex-matched wild-type mice (mean ± SEM; n = 5).

(B) The same organs were homogenized, and proteins were extracted by sonication. Following SDS–polyacrylamide gel electrophoresis, the amount of p27 was determined by immunoblot using carboxyl terminus–specific p27 antibodies. The top panel is from $p27^{+/+}$ mice and the bottom panel is from $p27^{-/-}$ mice. Molecular mass is indicated to the right of each panel.

to determine whether the absence of p27 affected the number of proliferating cells. We detected an increase in the number of splenic T cells in $p27^{-/-}$ mice (Table 1). This increase in T cell number might occur either during maturation in the thymus or following antigen exposure in the periphery.

To determine whether the $p27^{-/-}$ genotype affected thymocyte maturation, we examined the proportion of thymocytes at various stages of T cell development in mice (n = 8) by fluorescence-activated cell sorting. At each stage the number of cells was greater in $p27^{-/-}$ mice than in controls, although the percentage of cells was approximately equivalent with the possible exception of the $CD44^{+}CD25^{-}$ cells (Table 1). In one 8-week-old mouse, the percentage of $CD44^{+}CD25^{-}$ cells was increased 2-fold, although the other thymocyte subpopulations were not affected. $CD44^{+}CD25^{-}$ cells represent the earliest thymocyte stage we examined, and the biological significance of this result is not clear.

Thymocyte number is a function of the balance between cell proliferation and cell death. To detect thymocytes engaged in S phase, we measured the extent of bromodeoxyuridine (BrdU) incorporation into chromosomal DNA by immunohistochemistry following a single intraperitoneal injection of BrdU. We found an increase in the number of BrdU-positive thymocytes in thymus from $p27^{-/-}$ animals, in both the cortical region (Figures 5Ab and 5Ae) and the medullary region (Figures 5Aa and 5Ad). Moreover, this increase in the number of BrdU-positive cells was greater than could be accounted for by the increase in cell number. We quantified the percentage of BrdU-positive cells in random medullar fields of several sections. This analysis showed that the loss of p27 resulted in high levels of thymocyte proliferation. The mean percentage of BrdU-positive cells in three $p27^{+/+}$ mice was 10%, with values in random fields ranging from 3% to 19%. In contrast, the mean percentage of BrdU-positive cells in three $p27^{-/-}$ mice was 26%, with values ranging from 24% to 33%.

We did not detect a change in apoptosis using the TUNEL assay, which specifically labels nuclear DNA fragmentation (Gavrieli et al., 1992), on sections of the thymus (data not shown). To confirm that the sensitivity of $p27^{-/-}$ thymocytes to apoptosis was not changed, we measured the sensitivity of isolated thymocytes to apoptosis-inducing conditions, either γ-irradiation or dexamethasone. These treatments induced cell death in a similar percentage of $p27^{-/-}$ and control thymocytes (Figure 5B). Taken together, these data suggest that loss of p27 might increase the proportion of thymocytes engaged in the mitotic cycle.

We also determined whether mature T cells lacking p27 were more sensitive to antigen-induced proliferation. We activated splenic T cells by cross-linking the T cell receptor with increasing amounts of anti-CD3 antibody. For each amount of antibody, in the presence or absence of exogenous interleukin-2 (IL-2), the activation of $p27^{-/-}$ T cells was equivalent to the control (Figure 5C).

Female Mice Lacking Functional p27 Are Infertile

We found that $p27^{-/-}$ males could impregnate wild-type females; however, no $p27^{-/-}$ female carried pups to term. Specific female infertility could result from a variety of defects intrinsic to ovarian cells or of endocrine origin (or both).

Estrus is an indicator of endocrine function. Vaginal smears taken from 8- to 20-week-old mice showed that control mice passed though diestrus (day 1), proestrus (day 2), estrus (day 3), and metestrus (day 4) in 4 days (Figure 6) as described previously (Nelson et al., 1982). In contrast, all the $p27^{-/-}$ mice had prolonged estrus cycles, typically showing a prolongation prior to estrus and a delay in exiting estrus (Figure 6). Most characteristic was the diestrus–proestrus-like smear with numerous leukocytes and nucleated epithelial cells within abundant mucus. This smear type often was present for 5–7 days. After a short transition, a prolonged estrus phase followed and persisted for 4–5 days.

$p27^{-/-}$ female mice (n = 8) were capable of mating, albeit infrequently, as confirmed by formation of vaginal plugs; however, none of the mice maintained a pregnancy to the point where we could observe swelling of the abdomen. On day 3.5 after formation of the plug, we sacrificed 3-month-old females (n = 3) and isolated morula-stage embryos from these mice, indicating that

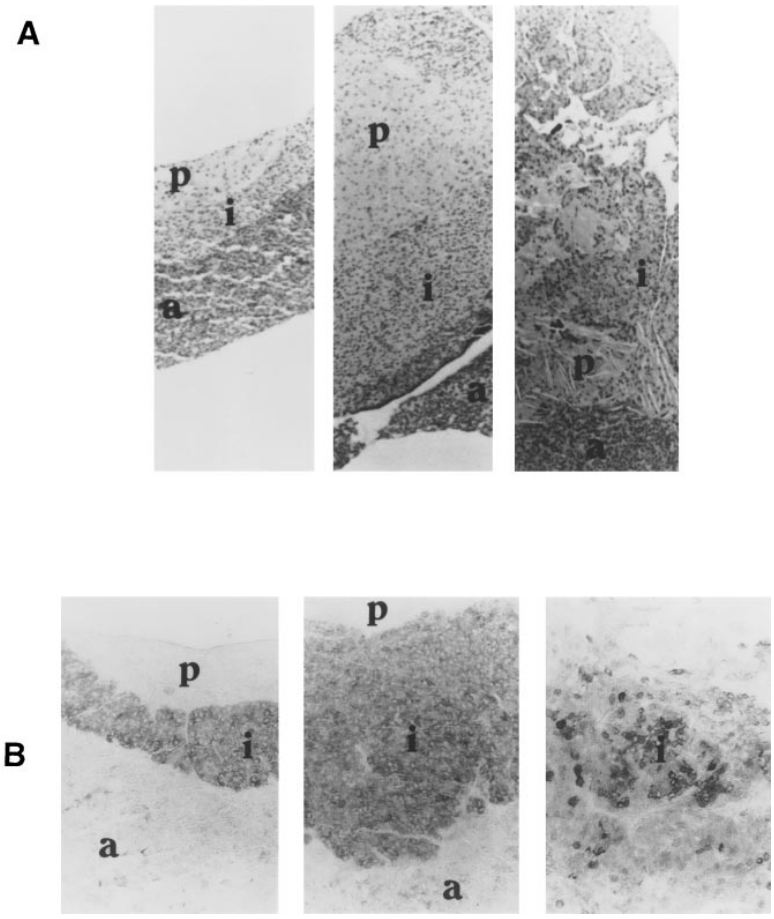

Figure 4. Intermediate Lobe Hyperplasia in $p27^{-/-}$ Mice

(A) $p27^{-/-}$ mice have enlarged pituitaries, which can be attributed to selective hyperplasia of the intermediate lobe. A composite picture comparing hematoxylin- and eosin-stained pituitary sections (top) from an 11-week-old $p27^{+/+}$ (left), an 11-week-old $p27^{-/-}$ (middle), and a 30-week-old $p27^{-/-}$ (right) mouse. p, posterior lobe; i, intermediate lobe; a, anterior lobe. The intermediate lobe of 11-week-old $p27^{-/-}$ mice is increased in size relative to the $p27^{+/+}$ controls, with little change in cellular composition. In 30-week-old $p27^{-/-}$ mice, the intermediate lobe is clearly hyperplastic with a nodular appearance, resulting in the disruption of the posterior lobe tissue. In both $p27^{-/-}$ mice the anterior lobe cells are compressed relative to the wild-type controls; however, the cell number does not appear to be altered.

(B) Intermediate lobe cells of $p27^{-/-}$ mice stain positively for POMC-derived peptides. Composite picture of pituitary sections stained by avidin–biotin horseradish peroxidase immunocytochemistry for POMC-derived peptides. In 11-week-old $p27^{+/+}$ (left) and $p27^{-/-}$ mice (middle) all intermediate lobe cells are uniformly stained, while intermediate lobe cells of 30-week-old $p27^{-/-}$ mice (right) display isolated and heterogeneous staining.

fertilization had occurred. Furthermore, these morula developed to full term when transferred to the oviducts of a pseudopregnant normal female. This suggests that ovulation and fertilization do occur in $p27^{-/-}$ mice and oocyte development itself does not require p27.

The disordered estrus cycle might reflect an underlying problem in endocrine signaling between the pituitary and ovary. To determine if the ovaries of the $p27^{-/-}$ mice would respond to exogenous gonadotropin stimulation similarly to controls, we injected 3- to 5-week-old mice ($n = 6$) with a follicle-stimulating hormone (FSH) preparation, pregnant mare serum, and 48 hr later with a luteinizing hormone (LH) substitute, human chorionic gonadotropin (HCG), and observed the effect on ovulation. This treatment greatly exaggerates the levels and sequential nature of the endogenous hormones. Under these conditions, we confirmed ovulation in both $p27^{+/+}$ (5 of 6) and $p27^{-/-}$ mice (4 of 6) by microscopic analysis of cells flushed from the oviducts 24 hr after HCG injection.

The infertility of $p27^{-/-}$ females might be due not only to irregular ovulation, but also to defects in the ability to maintain an environment suitable to maintain pregnancy. Corpus luteum formation plays an important role in maintenance of pregnancy by actively secreting progesterone and other factors. Granulosa cells, the major somatic cell component of follicles, differentiate into progesterone-producing luteal cells following ovulation. To determine if p27 was involved in luteal cell differentia-

Table 1. Comparison of Thymocyte Cell Number in $p27^{+/+}$ and $p27^{-/-}$ Mice

Cell Type	Cell Number (10^6)		Fold Increase in Cell Number Attributed to p27 Gene Disruption	Percent of Population	
	+/+	−/−		+/+	−/−
Total splenic T cells	34.20	63.57	1.9		
Total thymocyte	176.67	480.00	2.7		
$CD44^+CD25^-$	0.33	1.51	3.1	0.19	0.31
$CD44^+CD25^+$	0.08	0.25	2.6	0.05	0.05
$CD44^{lo}CD25^+$	1.62	4.18	2.6	0.88	0.78
$CD44^{lo}CD25^-$	1.87	4.89	2.7	1.06	1.02
$CD4^+CD8^+$	154.27	423.03	2.5	87.30	88.11
$CD4^+CD8^-$	13.54	33.75	2.5	7.68	7.03
$CD4^-CD8^+$	4.98	12.53	2.7	2.82	2.61

Numbers represent the mean of three independent experiments.

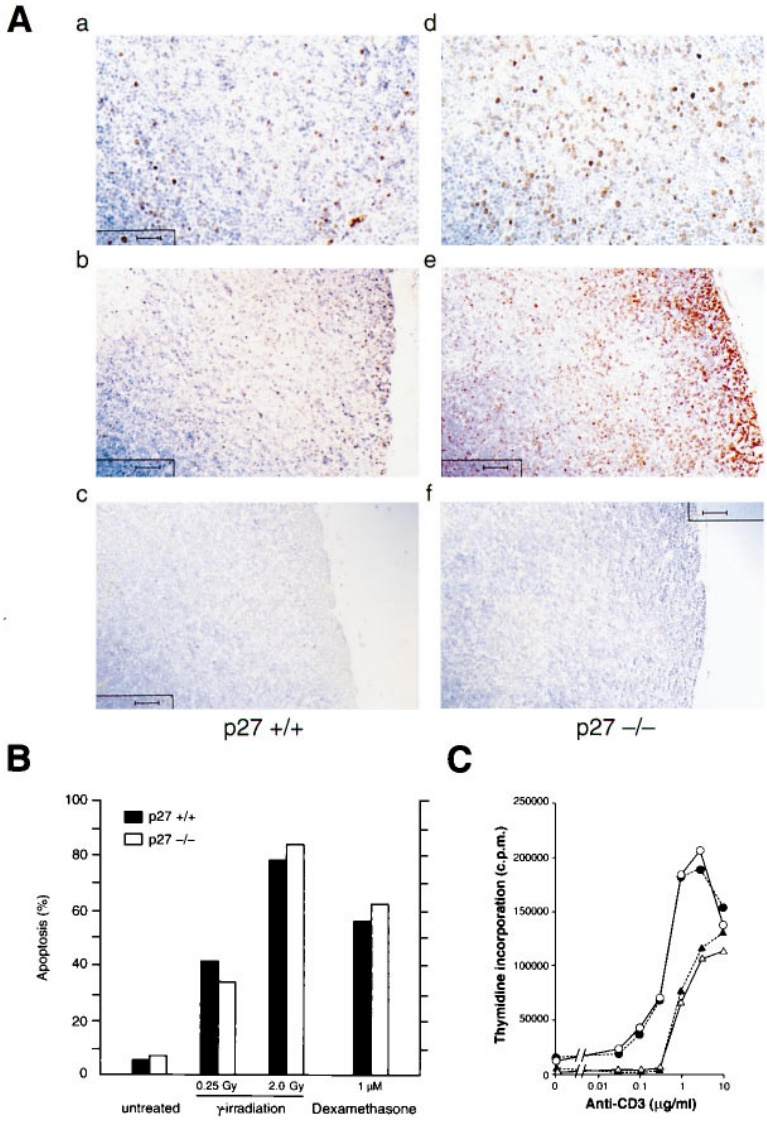

Figure 5. Increased Proliferation of Thymocytes Accounts for the Increase in T Cell Number

(A) The proportion of thymocytes in S phase is increased in $p27^{-/-}$ mice. Mice (4 weeks old) were labeled with BrdU for 2 hr, and incorporation into thymocytes was determined by anti-BrdU antibody staining. Sections of thymus isolated from either $p27^{+/+}$ (a–c) or $p27^{-/-}$ (d–f) mice are shown. In (a) and (d), the scale bar corresponds to 100 μm; in (b) and (e), the scale bar corresponds to 50 μm. (c) and (f) are the same as (b) and (e), but anti-BrdU antibody was omitted.

(B) Thymocytes of the $p27^{-/-}$ mice are susceptible to apoptosis. An example of two independent experiments is shown. Thymocytes were isolated from mice and exposed to either 0.25 or 5 Gy of irradiation or 1 μM dexamethasone, as indicated below each sample. Apoptotic cells were detected by the appearance of acridine orange–stained condensed or fragmented chromatin and plotted as a percent of the total cells. $p27^{+/+}$, closed bars; $p27^{-/-}$, open bars.

(C) T cell activation by anti-CD3 antibody is not affected by genotype. Thymidine incorporation (Y axis) was measured 72 hr after treatment with different concentrations of anti-CD3 (X axis) in the presence or absence of interleukin-2 (IL-2). $p27^{+/+}$, closed symbols; $p27^{-/-}$, open symbols. Circles, with IL-2; triangles, without IL-2.

tion, we examined the expression of p27 by immunohistochemistry. In control mice, p27 protein was undetectable in the granulosa cells of the follicle, but was abundant in the cells of the corpus luteum (Figure 7A, left). We observed a reciprocal pattern of BrdU staining: incorporation was highest in the follicular granulosa cells and lowest in luteal cells (Figure 7A, middle). Examination of $p27^{-/-}$ ovaries indicated defective formation of corpus luteum (Figure 7B). These data suggest that the absence of p27 might affect the transition from proliferating granulosa cell to nonproliferating luteal cell.

Discussion

p27 might have a function central to control of cell proliferation and, in turn, to animal growth. In animals, both complex regulatory signaling networks between cell types and intrinsic responses of cells to particular signals determine phenotype. Here we report that loss of p27 function as an inhibitor of G1 CDKs affects the response of cells to environmental signals, resulting in increased body growth. p27 disruption also appears to alter endocrine signaling by affecting the cells involved in the hypothalamic–pituitary–ovarian axis.

Evidence from previous studies suggests that p27 might establish an inhibitory threshold, set in part by mitogenic and anti-mitogenic signaling, that G1 CDKs must surpass before activation and entry into S phase (Sherr and Roberts, 1995; Koff and Polyak, 1995). Furthermore, the biochemical properties of p27 make it attractive to speculate that it might be responsible for establishing the balance between proliferating and nonproliferating cells. For these reasons, we decided to examine the role of p27 in proliferation and differentiation using a mouse model.

Disruption of p27 Affects the Manner in Which Cells Respond to Extracellular Signals to Proliferate or Withdraw from the Cell Cycle

As part of an inhibitory threshold, p27 might antagonize the S phase–promoting effect of CDKs and affect the

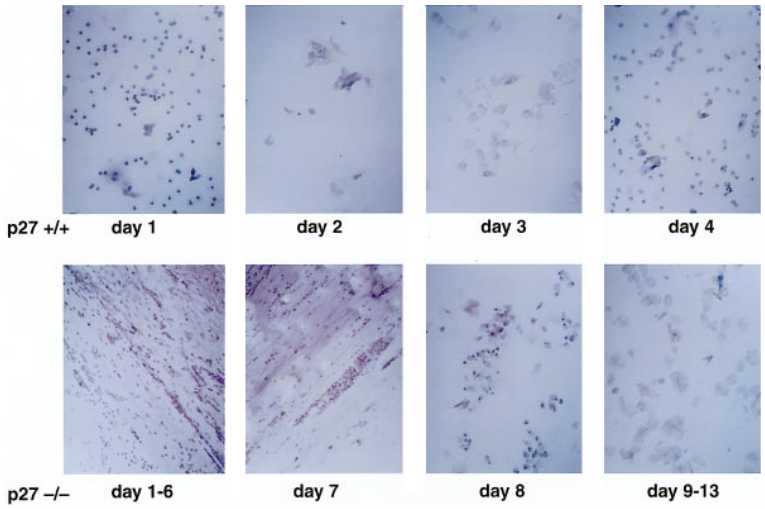

Figure 6. Estrus Is Perturbed in $p27^{-/-}$ Mice
Vaginal smears were obtained daily from $p27^{+/+}$ (top) or $p27^{-/-}$ (bottom) mice and stained with hematoxylin and eosin as described previously (Nelson et al., 1982). $p27^{+/+}$ mice complete estrus in 4 days, passing through diestrus, proestrus, estrus, and metestrus each in a single day (top row, left to right). $p27^{-/-}$ mice have a prolonged diestrus and estrus phases, and there is an increase in the amount of mucus during diestrus phase of the $p27^{-/-}$ mice.

decision to proliferate or withdraw from the mitotic cycle. In animals, exposure of a cell to mitogenic and anti-mitogenic signals is rarely an all or nothing event, although the cell makes an irrevocable choice in response to these signals. Anti-mitogens induce both rapid and slow responses in cells. Exposure either of HL60 cells to 12-O-tetradecanoylphorbol-13-acetate (TPA) (J. S. Yan, H. K., and A. K., unpublished data) or of Mv1Lu cells to transforming growth factor β (Ewen et al., 1993; Polyak et al., 1994a; Slingerland et al., 1994; Reynisdottir et al., 1995) rapidly induces CDK inhibitors and, more slowly, a decrease in the amount of cyclin and CDK proteins. If these signaling pathways target both events, the loss of p27 might not qualitatively prevent withdrawal from the mitotic cycle, but would affect the quality of the response.

We found that disruption of p27 affects the balance between proliferating and nonproliferating cells in the animal. We have shown directly that there is an increase in the fraction of S phase cells in $p27^{-/-}$ thymus. This effect of p27 gene disruption might be largely restricted to tissues undergoing postnatal maturation and reconstitution. Further analysis during embryogenesis will be required to address this. In agreement with Nakayama and colleagues (1996 [this issue of *Cell*]), we observed disorder of the regular array of the retina in $p27^{-/-}$ mice, although penetrance was incomplete (data not shown). This disorder may arise as a consequence of an unbalanced increase in the number of a particular type of cell in this normally highly organized tissue. In addition, an alteration in the ability of cells to withdraw from the cell cycle is suggested by the absence of corpus luteum in $p27^{-/-}$ mice. Luteal cell differentiation is accompanied by an increase in the amount of p27, and the granulosa cell that is unable to express p27 might either be trapped in the cell cycle and unable to differentiate, withdrawn from the cell cycle but unable to differentiate, or undergoing apoptosis.

Thus, we interpret some of the phenotypes of the $p27^{-/-}$ mice as a reduction in the capability of cells to respond to outside signals, either mitogenic or anti-mitogenic, which is consistent with an inhibitory threshold role based on the biochemical properties of p27. However, most developmental programs in the $p27^{-/-}$ mouse do succeed because specialized organs form and mice are viable. This is consistent with observations that $p27^{-/-}$ MEFs arrest when deprived of serum or grown to confluence and, when released from quiescence, reenter S phase and activate CDK2 with kinetics similar to controls (unpublished data). This suggests that p27 might regulate withdrawal from the mitotic cycle dependent on the type of signals the cell receives and the type of redundant response the signal might elicit in the cell.

Hyperplasia of the Intermediate Lobe of the Pituitary Suggests That p27 Might Maintain Cells in a Nonproliferative State

The disruption of p27 gives rise to intermediate lobe pituitary hyperplasia without evidence of adenoma (up to 30 weeks). Although all cells are originally αMSH positive, the staining in the hyperplastic nodules is variable. We speculate that p27 might be required to maintain these cells in a nonproliferative, differentiated state. The significance of hyperplasia restricted to these cells is unclear. Mice that have lost heterozygosity at the *Rb* locus develop adenoma of the intermediate lobe (Jacks et al., 1992; Hu et al., 1994). Perhaps these cells are exquisitely sensitive to the loss of negative regulators of cell cycle progression. One possibility is that these highly differentiated cells might retain the capacity to undergo postnatal reconstitution. In addition, this observation suggests that p27 and Rb might be in the same genetic pathway regulating proliferation of these cells. This is consistent with the findings that CDK phosphorylation of Rb decreases its ability to suppress growth (Hinds et al., 1992). Hyperplasia, rather than adenoma, might occur in $p27^{-/-}$ mice either because of redundancy of regulation at the level of CDK activity or because the loss of the p27-inhibitory pathway might not be sufficient

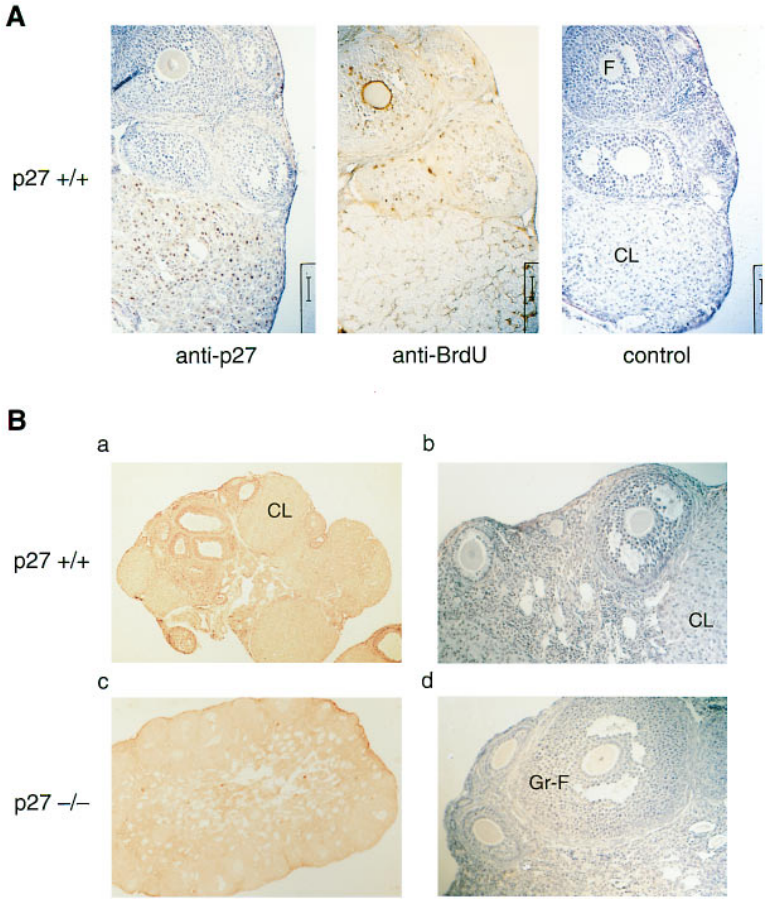

Figure 7. p27$^{-/-}$ Mice Are Deficient in Corpus Luteum Formation

(A) There is a reciprocal pattern of staining with p27- and BrdU-specific antibodies in the ovaries of p27$^{+/+}$ mice. Ovaries from mice labeled with BrdU were isolated, sectioned, and stained with either anti-p27, anti-BrdU, or a rabbit immunoglobulin control antibody, as indicated below each panel. This antibody was detected with a secondary antibody conjugated to horseradish peroxidase. p27 protein is expressed in luteal cells. Granulosa cells incorporate BrdU. Magnification is approximately 60×, and the scale bar corresponds to 50 μm.

(B) Ovaries of the p27$^{-/-}$ mice lack the highly differentiated corpus luteum structure observed in controls. Composite picture comparing the ovaries of p27$^{+/+}$ (top) and p27$^{-/-}$ (bottom) mice by hematoxylin and eosin staining. Magnifications are approximately 15× and 60× (left and right, respectively). Mature follicles are present in both animals. CL, corpus luteum; GF, Graafian follicle; F, follicle.

to obviate all the properties of Rb that make it a tumor suppressor.

Female Fertility Defects Implicate Changes in the Nature of Endocrine Signaling in p27$^{-/-}$ Mice

Alteration in the fate of cell proliferation might affect signaling between organs. A complex temporal hormonal network regulates estrus. Expression of gonadotropin-releasing hormone leads to gonadotrope release of FSH and LH. FSH interacts with ovarian granulosa and theca cells and induces expression of estrogen synthetic enzymes and LH receptors. Later during the estrus cycle, the LH receptor–expressing granulosa cells respond to pulsatile LH secretion, and ovulation follows a short time later. The remnant follicle composed of granulosa cells subsequently undergoes differentiation into progesterone- and estrogen-producing luteal cells. If the oocyte is not fertilized, the corpus luteum disintegrates and a new cycle begins. We interpret the estrus phenotype of the p27$^{-/-}$ mouse to reflect perturbation of endocrine signaling networks between the ovary and the pituitary.

At this time we can speculate that in p27$^{-/-}$ mice signaling between the ovary and the pituitary is compromised; however, further work is required to determine the mechanism by which intermediate lobe hyperplasia, the perturbed estrus cycle, and luteal cell differentiation are linked. Hyperplasia might interfere directly or indirectly with other endocrine networks that modulate the gonadotropin-releasing hormone–FSH–LH axis. Perhaps more important is the inability to form a corpus luteum and its potential effects on endocrine pathways. Hormones, produced in the luteal cells such as inhibin and relaxin, might regulate pituitary function. The prolonged estrus phase might be a reflection of corpus luteum dysfunction, because initiation of the next estrus cycle requires completion of the previous cycle, either by corpus maintenance or corpus disintegation. Consequently, the endocrine defect might be, at least in part, due to the inability of granulosa cells to differentiate properly into luteal cells, although the involvement of the pituitary as a primary factor cannot be ruled out.

Enhanced Growth of Mice with Disrupted p27 Alleles Reflects Its Function as an Intracellular Regulator of Proliferation

As in ovulation, a complex endocrine network regulates growth. GH-releasing hormone and somatostatin regulate the somatotropes that secrete GH. GH induces IGF-I production, and IGF-I increases protein synthesis and mitogenesis in target cells. Transgenic mice expressing either GH or IGF-I grow to a larger size than control animals (Palmiter et al., 1982; Mathews et al., 1988). The GH–IGF-I hormonal axis does not play a major role in the p27$^{-/-}$ growth phenotype, because the number of

somatotropes and the amount of stored GH appear identical in $p27^{-/-}$ and control animals and there is no increase in the level of serum IGF-I.

We speculate that the increase in mitotic cells before maturation of an organ might in part explain increased growth of the animal. First, p27 gene disruption results in an increase in the proportion of cycling cells and cell number. Second, the growth of $p27^{-/-}$ mice was a function of p27 gene copy number and p27 protein expression. $p27^{-/-}$ mice were significantly larger than $p27^{+/-}$ mice, which were in turn larger than wild-type littermates. The thymus and spleen, which in control animals express the highest amounts of p27, were significantly increased in weight, whereas organs that normally express lower levels of p27 were less affected by its disruption. Third, we observed that embryonic fibroblasts and splenic T cells isolated from $p27^{-/-}$ mice are partially resistant to the anti-proliferative effects of rapamycin at low concentrations (unpublished data). These data suggest that p27 disruption might affect animal growth in part by altering the balance between proliferating and nonproliferating cells at critical periods of development, which might vary for each organ.

We speculate that p27 acts as a true regulator of growth by exerting its actions on the decision of a cell either to proliferate or to withdraw from the cell cycle in response to environmental signals. In single-cell eukaryotes and cells of vertebrate origin, growth is an accumulation of sufficient cell mass (Prescott, 1976). However, growth of an animal is due, in part, to a net increase in the number of cells. Accordingly, p27 might have a central function, albeit partially redundant, in the control of cell proliferation and, in turn, in enhancing animal growth.

Experimental Procedures

Targeted Mutagenesis in the Mouse p27 Gene

We isolated the mouse p27 gene by screening a 129 mouse genomic library (Stratagene) using the total coding region of mouse p27 cDNA as a probe. A 6.0 kb BamHI fragment that contained the protein-coding sequence, exons 1 and 2, was subcloned into a pBS vector. We cleaved this construct at a SmaI site located in codon 42 of exon 1 by partial digestion and inserted a 1.1 kb blunt-ended XhoI–BamHI fragment encoding pMC-1–neo–poly(A) (Stratagene). We subsequently digested with NotI and BamHI and inserted a 1.2 kb herpes simplex virus TK gene cassette driven by the polyoma enhancer.

NotI-linearized targeting vector was introduced into CJ7 ES cells by electroporation (Swiatek and Gridley, 1993). Positively transfected cells were selected in 0.5 mg/ml G418 and 0.2 μM ganciclovir. We analyzed their genotype at the p27 locus by Southern blotting following EcoRI digestion. The 1.1 kb EcoRI–BamHI fragment 5′ to the vector fragment was used as a probe as shown (Figure 1B).

We microinjected p27 heterozygous ES cells into blastocyst-stage C57BL/6 mouse embryos. We transplanted injected blastocysts into uteri of pseudopregnant C57BL/6 mice. Chimeric males were crossed to C57BL/6 females. We monitored germline transmission of the injected ES cells by detecting agouti mice among the F1 offspring and subsequent Southern blotting, as described above.

Cell Culture and Protein Analysis

Embryonic fibroblasts were obtained from day-13.5 embryos. To prepare extracts, we lysed cells by sonication in Rb kinase lysis buffer (Soos et al., 1996) and determined protein content by Bradford assay. p27 was detected with either affinity-purified antibody or a carboxyl terminus–specific antibody as described elsewhere (Soos et al., 1996). Antibodies specific for the carboxyl terminus of p27, CDK2, and CDK4 were obtained from Santa Cruz Biotechnology.

Preparation of Recombinant Proteins and Kinase Assays

His-tagged versions of wild-type p27 and Δ51 were expressed in bacteria and purified by metal affinity chromatography (Polyak et al., 1994b). Rb kinase experiments using baculovirus-encoded cyclins and CDKs were performed as described previously (Polyak et al., 1994b). We measured the incorporation of [γ-^{32}P]ATP into glutathione S-transferase–Rb fusion protein by phosphoimager (Fuji).

IGF-I Measurements

We used six littermate pairs of animals for this analysis. We also included three nonlittermate animals that were age matched. We obtained serum from each animal at two different ages and divided these into two groups, those collected from 6- to 10-week-old mice ($n = 13$) and those collected from 11- to 30-week-old mice ($n = 14$). IGF-I was measured by a double antibody RIA using recombinant human IGF-I (Genentech) and anti–human IGF-I serum UBK487 (National Hormone and Pituitary Program, National Institutes of Health) after removal of binding proteins from a 5 μl aliqot of serum by means of a Sep-Pak C18 reverse phase cartridge (Millipore). We compared the amount of IGF-I in $p27^{+/+}$ and $p27^{-/-}$ mice in the following ways: all sex matched, age and sex matched, and all age matched. We also included two other comparisons that focused only on the age and sex of the animal and not the genotype: all females compared to all males and all age matched. There were no statistically significant differences between any group except for the comparison of male and female mice regardless of genotype ($t = 2.044$; $p < 0.05$).

Histology

Tissues, with the exception of the pituitary, were fixed in 4% paraformaldehyde at 4°C overnight, dehydrated with ethanol, embedded in paraffin, and sectioned at 4 μm. The sections were used for hematoxylin–eosin staining or immunohistochemistry as indicated in the figure legends.

To detect proliferating cells, we injected mice intraperitoneally (50 μg per gram of body weight) with BrdU (Morstyn et al., 1983). We sacrificed the mice 2 hr later, isolated thymus and ovaries, and prepared the tissues for sectioning. After successive treatment with proteinase K, 1N HCl, and 0.1% H_2O_2, we blocked slides with the avidin–biotin blocking solution (Vector) and incubated slides overnight at 4°C in blocking buffer (10% horse serum, 2% BSA, 0.5% Tween 20) containing 6 μg/ml anti-BrdU monoclonal antibody (Boerhinger Mannheim). We subsequently detected antibody binding with biotinylated secondary antibody (1:200 dilution) and a peroxidase-conjugated streptavidin according to the instructions of the manufacturer (Vectastain).

To detect p27 in sections from ovaries, we used either affinity-purified antibody or the carboxyl terminus–specific antibody. The specificity was confirmed by using antibodies preincubated with an excess of antigen before staining.

We measured thymocyte apoptosis as described previously (Lowe et al., 1993; Clarke et al., 1993). For irradiation, we exposed thymocytes to γ-rays from a ^{137}Cs source at 0.1 Gy per minute. Following irradiation, we cultured cells in DMEM supplemented with 5% fetal calf serum for 8 hr. We subsequently fixed the cells to glass slides with acetic acid–ethanol solution (1:9) overnight. Fixed slides were treated sequentially with PBS, 0.1% Triton X-100, 0.08N HCl–0.15 M NaCl and subsequently stained with 20 μM acridine orange (Sigma) in a phosphate–citric acid buffer (pH 6) containing 1 mM EDTA and 0.15 M NaCl. Cells were examined in a fluorescence microscope, and apoptosis was determined by the presence of condensed or fragmented chromatin.

Pituitaries were fixed in 10% neutral buffered formalin. Sections were treated sequentially with 0.3% H_2O_2 in methanol, 1.5% normal goat serum, rabbit anti–human ACTH sera (1:10,000; National Institutes of Health), or monkey anti–rat GH sera (1:50,000; LAF 82469). Antibody binding was detected as described above. Replacement of the primary immune serum with normal rabbit or monkey serum abolished staining. Specificity of each antiserum was confirmed by

preabsorbtion of antibody with the respective antigen (1 μg/ml dilute primary antibody).

Fluorescence-Activated Cell Sorting

We made single-cell suspensions from the thymus and stained thymocytes as described previously (Wilson et al., 1988; Dudley et al., 1994).

Lymphocyte Activation

We obtained spleen cells by pressing the spleen against the bottom of a tissue culture dish with a bent syringe needle. We collected cells by centrifugation and lysed erythrocytes. The remaining cells were centrifuged through FBS, washed with PBS, and resuspended in growth media with RPMI 1640 plus 10% FBS, 2 mM glutamine, nonessential amino acids, 1 mM sodium pyruvate, and 50 μM 2-mercaptoethanol. To eliminate B lymphocytes, we added anti-B220 antibody and incubated at 4°C for 1 hr and then added rabbit serum complement and continued the incubation for 45 min at 37°C. Cells that did not adhere to the flask during incubation were collected and washed extensively. More than 80% of the resulting cells were T lymphocytes. We subcultured 2×10^5 viable cells for 72 hr in 0.5 ml of medium containing various amounts of anti-CD3 antibody with or without 100 U/ml IL-2. [^{3}H]thymidine (2 mCi/mmol, 1 μCi per sample) was added for the last 4 hr of the culture. The labeled cells were harvested, and incorporated [^{3}H]thymidine was measured by liquid scintillation counter.

Acknowledgements

Correspondence should be addressed to A. K. We thank Joan Massagué and Kornelia Polyak for providing the p27*Kip1* cDNA prior to publication and David Morgan and Charles Sherr for baculoviruses encoding cyclins and CDKs. We are grateful for the helpful discussions and advice of Arch Perkins, Pier Paolo Pandolfi, Elizabeth Lacy, Lee Niswander, Roberta Rivi, Roger Pearse, Steve Swendeman, and our other colleagues at the institutes. We thank James Roberts and Kei-ichi Nakayama for communicating results prior to publication. We thank Birming Wong, Jia-Hui Dong, Karen Witty-Blease, Steve Bottega, Timothy J. Soos, Tom Taylor, and Michael Butz for excellent technical assistance. We thank Chris Fisher, Lee Niswander, and Joan Massagué, for critical reading of the manuscript. This work was supported by grants from the National Institutes of Health to A. K. (GM52597), L. A. F. (NIDDK30667), and A. C. H. (GM37759), The Society of Memorial Sloan–Kettering Cancer Center to A. K., and The Bane Foundation to L. A. F. and a grant from the National Cancer Insititute to Memorial Sloan–Kettering Cancer Center. H. K. is supported by the DeWitt Wallace Research Fund of Memorial Sloan–Kettering Cancer Center.

Received March 7, 1996; revised April 16, 1996.

References

Chen, I.-T., Akamatsu, M., Smith, M.L., Lung, F.-D.L., Duba, D., Roleer, P.P., Fornace, A.J., Jr., and O'Connor, P.M. (1996). Characterization of p21 Cip1/Waf1 peptide domains required for cyclin E/Cdk2 and PCNA interaction. Oncogene *12*, 595–607.

Clarke, A.R., Purdie, C.A., Harrison, D.J., Morris, R.G., Bird, C.C., Hooper, M.L., and Wylie, A.H. (1993). Thymocyte apoptosis induced by p53-dependent and independent pathways. Nature *362*, 849–852.

Coats, S., Flannagan, W., Nourse, J., and Roberts, J.M. (1996). Requirement of p27Kip1 for restriction point control of the fibroblast cell cycle. Science, in press.

Dudley, E.C., Petrie, H.T., Shah, L.M., Owen, M.J., and Hayday, A.C. (1994). T cell receptor β chain gene rearrangment and selection during thymocyte development in adult mice. Immunity *1*, 83–93.

Ewen, M.E., Sluss, H.K., Whitehouse, L.L., and Livingston, D.M. (1993). TGFβ inhibition of CDK4 synthesis is linked to cell cycle arrest. Cell *74*, 1009–1020.

Gavrieli, Y., Sherman, Y., and Ben-Sasson, S.A. (1992). Identification of programmed cell death *in situ* via specific labeling of nuclear DNA fragmentation. J. Cell Biol. *119*, 493–501.

Gu, Y., Turck, C.W., and Morgan, D.O. (1993). Inhibition of CDK2 activity *in vivo* by an associated 20K regulatory subunit. Nature *366*, 707–710.

Harper, J.W., Adami, G.R., Wei, N., Keyomarsi, K., and Elledge, S.J. (1993). The p21 Cdk-interacting protein Cip1 is a potent inhibitor of G1 cyclin-dependent kinases. Cell *75*, 805–816.

Harper, J.W., Elledge, S.J., Keyomarsi, K., Dynlacht, B., Tsai, L.H., Zhang, P., Dobrowolski, S., Bai, C., Connell-Crowley, L., Swindell, E., Fox, M.P., and Wei, N. (1995). Inhibition of cyclin-dependent kinases by p21. Mol. Biol. Cell *6*, 387–400.

Hinds, P.W., Mittnacht, S., Dulic, V., Arnold, A., Reed, S.I., and Weinberg, R.A. (1992). Regulation of retinoblastoma functions by ectopic expression of human cyclins. Cell *70*, 993–1006.

Hu, N., Gutsmann, A., Herbert, D.C., Bradley, A., Lee, W.H., and Lee, E.Y.-H.P. (1994). Heterozygous Rb-1$^{\Delta 20/+}$ mice are predisposed to tumors of the pituitary gland with a nearly complete penetrance. Oncogene *9*, 1021–1027.

Jacks, T., Fazeli, A., Schmitt, E.M., Bronson, R.T., Goodell, M.A., and Weinberg, R.A. (1992). Effects of an *Rb* mutation in the mouse. Nature *359*, 295–300.

Koff, A., and Polyak, K. (1995). p27KIP1, an inhibitor of cyclin-dependent kinases. In Progress in Cell Cycle Research, Volume 1, L. Meijer, S. Guidet, and H.Y.L. Tung, eds. (New York: Plenum Press), pp. 141–147.

Kranenburg, O., Scharnhorst, V., Van der Eb, A., and Zantema, A. (1995). Inhibition of cyclin-dependent kinase activity triggers neuronal differentiation of mouse neuroblastoma cells. J. Cell Biol. *131*, 227–234.

Lee, M.H., Reynisdottir, I., and Massagué, J. (1995). Cloning of p57KIP2, a cyclin-dependent kinase inhibitor with a unique domain structure and tissue distribution. Genes Dev. *9*, 639–649.

Liu, M., Lee, M.H., Cohen, M., Bommakanti, M., and Freedman, L.P. (1996). Transcriptional activation of the Cdk inhibitor p21 by vitamin D3 leads to the induced differentiation of the myelomonocytic cell line U937. Genes Dev. *10*, 142–153.

Lowe, S.W., Schmitt, E.M., Smith, S.W., Osborne, B.A., and Jacks, T. (1993). p53 is required for radiation-induced apoptosis in mouse thymocytes. Nature *362*, 847–849.

Luo, Y., Hurwitz, J., and Massagué, J. (1995). Cell-cycle inhibition by independent CDK and PCNA binding domains in p21Cip1. Nature *375*, 159–161.

Mansour, S.L., Thomas, K.R., and Capecchi, M.R. (1988). Disruption of the proto-oncogene int-2 in mouse embryo-derived stem cells: a general strategy for targeting mutations to non-selectable genes. Nature *366*, 348–354.

Mathews, L.S., Hammer, R.E., Behringer, R.R., D'Ercole, A.J., Bell, G.I., Brinster, R.L., and Palmiter, R.D. (1988). Growth enhancement of transgenic mice expressing human insulin-like growth factor I. Endocrinology *123*, 2827–2833.

Matsuoka, S., Edwards, M.C., Bai, C., Parker, S., Zhang, P., Baldini, A., Harper, J.W., and Elledge, S.J. (1995). p57KIP2, a structurally distinct member of the p21CIP1 Cdk inhibitor family, is a candidate tumor suppressor gene. Genes Dev. *9*, 650–662.

Morgan, D.O. (1995). Principles of CDK regulation. Nature *374*, 131–134.

Morstyn, G., Hsu, S.M., Kinsella, T., Gratzner, H., Russo, A., and Mitchell, J.B. (1983). Bromodeoxyuridine in tumors and chromosomes detected with a monoclonal antibody. J. Clin. Invest. *72*, 1877–1883.

Nakanishi, M., Robetoyre, R.S., Adami, G.R., Pereira-Smith, O.M., and Smith, J.R. (1995). Identification of the active region of the DNA synthesis inhibitory gene p21Sdi1/CIP1/WAF1. EMBO J. *14*, 555–563.

Nakayama, K., Ishida, N., Shirane, M., Inomata, A., Inoue, T., Shishido, N., Horii, I., Loh, D.Y., and Nakayama, K.-i. (1996). Mice lacking p27*Kip1* display increased body size, multiple organ hyperplasia, retinal dysplasia, and pituitary tumors. Cell *85*, this issue.

Nelson, J.F., Felicio, L.S., Randall, P.K., Sims, C., and Finch, C.B. (1982). A longitudinal study of estrous cyclicity in aging C57BL/6J

mice. I. Cycle frequency, length, and vaginal cytology. Biol. Reprod. *27*, 327–339.

Ohtsubo, M., and Roberts, J.M. (1993). Cyclin-dependent regulation of G1 in mammalian fibroblasts. Science *259*, 1908–1912.

Palmiter, R.D., Brinster, R.L., Hammer, R.E., Trumbauer, M.E., Rosenfeld, M.G., Brinberg, N.C., and Evans, R.M. (1982). Dramatic growth of mice that develop from eggs microinjected with metallothionein-growth hormone fusion genes. Nature *300*, 611–615.

Pardee, A.B. (1989). G1 events and the regulation of cell proliferation. Science *246*, 603–608.

Polyak, K., Kato, J.Y., Solomon, M.J., Sherr, C.J., Massagué, J., Roberts, J.M., and Koff, A. (1994a). $p27^{KIP1}$, a cyclin-Cdk inhibitor, links transforming growth factor-β and contact inhibition to cell cycle arrest. Genes Dev. *8*, 9–22.

Polyak, K., Lee, M.-H., Erdjument-Bromage, H., Koff, A., Roberts, J.M., Tempst, P., and Massagué, J. (1994b). Cloning of p27*Kip1*, a cyclin-dependent kinase inhibitor and a potential mediator of extracellular antimitogenic signals. Cell *78*, 59–66.

Prescott, D.M. (1976). Reproduction of Eukaryotic Cells (New York: Academic Press).

Quelle, D.E., Ashmun, R.A., Shurtleff, S.A., Kato, J.Y., Bar-Sagi, D., Roussel, M.F., and Sherr, C.J. (1993). Overexpression of mouse D-type cyclins accelerates G1 phase in rodent fibroblasts. Genes Dev. *7*, 1559–1571.

Resnitzky, D., and Reed, S.I. (1995). Different roles for cyclin D1 and E in regulation of the G1-to-S transition. Mol. Cell. Biol. *15*, 3463–3469.

Reynisdottir, I., Polyak, K., Iavarone, A., and Massagué, J. (1995). Kip/Cip and Ink4 Cdk inhibitors cooperate to induce cell cycle arrest in response to TGF-β. Genes Dev. *9*, 1831–1845.

Sherr, C.J. (1993). Mammalian G1 cyclins. Cell *73*, 1059–1065.

Sherr, C.J., and Roberts, J.M. (1995). Inhibitors of mammalian G1 cyclin-dependent kinases. Genes Dev. *9*, 1149–1163.

Slingerland, J.M., Hengst, L., Pan, C.H., Alexander, D., Stampfer, M.R., and Reed, S.I. (1994). A novel inhibitor of cyclin-Cdk activity detected in transforming growth factor β-arrested epithelial cells. Mol. Cell. Biol. *14*, 3683–3694.

Soos, T.J., Kiyokawa, H., Yan, J.S., Rubin, M.S., Giordano, A., DeBlasio, A., Bottega, S., Wong, B., Mendelsohn, J., and Koff, A. (1996). Formation of p27-CDK complexes during the human cell cycle. Cell Growth Differ. *7*, 135–146.

Swiatek, P.J., and Gridley, T. (1993). Perinatal lethality and defects in hindbrain development in mice homozygous for a targeted mutation of the zinc finger gene Krox20. Genes Dev. *7*, 2071–2084.

Toyoshima, H., and Hunter, T. (1994). p27, a novel inhibitor of G1 cyclin–Cdk protein kinase activity, is related to p21. Cell *78*, 67–74.

Wilson, A., D'Amico, A., Ewing, T., Scollay, R., and Shortman, K. (1988). Subpopulations of early thymocytes: a cross correlation flow cytometric analysis of adult mouse Ly-2-L3T4 ($CD8^{-}CD4^{-}$) thymocytes using eight different surface markers. J. Immunol. *140*, 1461–1470.

Xiong, Y., Hannon, G.J., Zhang, H., Casso, D., Kobayashi, R., and Beach, D. (1993). p21 is a universal inhibitor of cyclin kinases. Nature *366*, 701–704.

Zhang, H., Hannon, G.J., and Beach, D. (1994). p21-containing cyclin kinases exist in both active and inactive states. Genes Dev. *8*, 1750–1758.